



Remediation of wastewaters from chlorophenol using agricultural wastes as adsorbents: adsorption, kinetics and chemical evaluation

Magdy F. El Ashry^a, Maher A. El Hashash^b, Nabel A. Negm^{c,*},
Maram T.H. Abou Kana^d, Mohamed A. Betiha^c

^aPetroleum Pipelines Company, Cairo, Egypt, email: magdy_fathy2002@yahoo.com

^bFaculty of Science, Ain Shams University, Cairo, Egypt, email: maher_elhashash@hotmail.com

^cEgyptian Petroleum Research Institute, Nasr city, Cairo, Egypt, emails: nabelnegm@hotmail.com (N.A. Negm), mohamed_betiha@hotmail.com (M.A. Betiha)

^dNational Institute of Laser Enhanced Sciences, Cairo University, Giza, Egypt, email: mabou202@hotmail.com

Received 10 April 2019; Accepted 14 August 2019

ABSTRACT

Phenolic compounds are mixtures of phenol derivatives which are produced from several industries including biocides, pharmaceuticals and coal production. Phenolics are considered the major contaminants in industrialized wastewater. Therefore, treatment of wastewater polluted by phenolics is mandatory previously to discharge in order to protect the environment. Among the numerous procedures reported for remediation of industrial wastewater from phenolics; adsorption technology was the best method from the effectiveness and economical point of view. In this study, three agricultural wastes produced in huge amounts were evaluated in remediation of wastewater contaminated by 2-chlorophenol. The studied agricultural wastes were water hyacinth, palm leaf, and banana peel. The adsorption process parameters were determined including temperature, pH, amount of adsorbents, concentration of pollutant, and treatment time. The process followed Freundlich adsorption isotherm and pseudo-second-order kinetic model. Boyd model showed that the adsorption mechanism of chlorophenol on the surface of the different adsorbents was occurred via film diffusion mechanism. The obtained adsorption capacities at the equilibrium conditions were 288.1, 290.3, and 388.9 mg/g for water hyacinth, palm leaf, and banana peel, respectively. The spectroscopic evaluation showed the physical interaction between the chlorophenol molecules and the different functional groups on the studied adsorbents. Banana peel showed the highest adsorption efficiency, which was related to the abundance and types of the bioactive compounds in its chemical structure.

Keywords: Chlorophenol; Remediation; Adsorption; Wastewater; Freundlich isotherm; Pseudo-second-order; Boyd model

1. Introduction

Phenolic compounds are presented in effluents of petroleum refineries, petrochemicals, plastics, coke production, and pharmaceutical industries [1–3]. Discharge of the untreated industrial wastes in the environment, for example, rivers, leads to severe health hazards to human, animals, and aquatic systems [1]. The US Environmental Protection

Agency (EPA) considered phenol as a substantial contaminant in industrial wastewater [1]. EPA regulations have set water purity standard of less than 1 ppb of phenol derivatives [2]. Phenolic compounds exhibit toxicity in the range of 9–25 mg/L for humans and aquatic systems [4]. Long-term contact for phenol derivatives leads to asymmetrical breathing, muscle defect, tremor, and respiratory defects in humans. Chronic contact to phenolics leads to irritation in the intestinal and central nervous systems [3,5,6]. Therefore,

* Corresponding author.

there is a necessity to eliminate phenolic compounds from wastewater before release. Conventional treatments such as distillation, chemical oxidation, and electrochemical oxidation show high efficiencies with various phenolic compounds, while progressive treatments such as ozonation, air oxidation, and photochemical treatment use less chemicals related to the conventional processes, but have high energy costs. Biological treatment is environmentally friendly and energy saving, but it cannot treat high concentration pollutants. Enzymatic treatment was the best way to treat various phenolic compounds under mild conditions using peroxidases, laccases, and tyrosinases. Chemical oxidation affords destructive remediation for phenolic compounds. The processes required less chemicals and consumes lower energy, operating under mild conditions of temperature and pH are most commonly in ppm range or higher. O_3 , Cl_2 , chlorine dioxide, chloramines, ferrate [Fe (VI)] and permanganate [MnO_4^-] are the common chemicals used in the oxidative treatment of phenol derivatives contaminated in wastewater [7]. Electrochemical oxidation is a destructive process of removal of phenol derivatives at which no chemicals are required, but required equipment and energy. As studied by Tasic et al. [8] and Ghimire et al. [9], electrochemical oxidation processes are of two types: direct and indirect oxidation. Direct or anodic process occurred by adsorption of the phenol derivatives on the anodic surface. Various anode materials are used such as Pt, PbO_2 , SnO_2 , IrO_2 , and boron-doped diamond. Biological treatment is the most commonly method in treatment for phenolic compounds. Bisphenol-A was removed using biological treatments such as activated sludge [10,11]. Enzymatic treatment takes its important from the biological treatment. In this process, biocatalyst (enzyme) is responsible for transformation on phenolic compounds into low toxic compounds or environmentally safe. The process has substantial advantages such as cost-effectiveness than conventional biological and chemical remediation, as long as the used enzymes are available and has economically price [12]. Adsorption process of organic materials from wastewater is an effective process due to the ability to remove a wide range of trace to percentage concentrations. Different adsorbents were showed their high efficiency in the removal of organic pollutants from the wastewater, especially the agricultural wastes [13,14]. Clays and modified clays also showed high percentage removal for different pollutants from wastewater including organics and heavy metal ions, dyes and organic compounds [15–17]. Modification of agricultural wastes into activated carbon had wide application in the field of pollutants remediation from the environment. Production of activated carbon is economically expensive, but it showed effective performance in removal of finite traces of various organic compounds [18,19]. New trends were developed including chemical modification of the activated carbon, impregnation with nanoparticles, different sources of carbon and activation methods [20–23].

In this study, three agricultural wastes were used in remediation of chlorophenol from wastewater. The effect of several parameters were determined on the adsorption process including the effect of adsorbent amount, chlorophenol concentration in the medium, time of adsorption process, pH of the medium and temperature using UV-Vis spectroscopic

measurements. Adsorption isotherms of the process were studied. Kinetics of the process also was studied using several kinetic models to determine the mechanism of the adsorption process. The rate determining step of the process was determined using Boyd model. The mechanism of the adsorption of chlorophenol on the different adsorbents was proposed based on the chemical structures of these adsorbents and the information obtained from the adsorption isotherms and kinetic studies.

2. Materials and methods

2.1. Chemicals

Stock solution of chlorophenol was prepared in deionized water using analytical grade chlorophenol obtained from Sigma-Aldrich, Germany (purity of 99.99%). Different concentrations of the chlorophenol solution were prepared by serial dilution of the stock solution using deionized water.

2.2. Adsorbents

In the remediation process, three adsorbents were tested namely: *Musa sapientum* (banana peel), palm leaf, and water hyacinth. The adsorbents were claimed, washed using bidistilled water dried to 50°C and crushed into fine particles of 1–2 mm diameter.

2.3. Measurements

The concentration of the remaining chlorophenol after each treatment was determined using Camspec M501 UV-Vis spectrophotometer at. A calibration curve of chlorophenol in bidistilled water was drawn at $\lambda = 290$ nm and a concentration range of 1–15 mg (2-chlorophenol)/mL (H_2O). The concentration of the remaining chlorophenol after each adsorption experiment was determined using the corresponding intensity at the characteristic wavelength. FTIR spectra of the studied adsorbents were performed before and after the adsorption process using Genesis Fourier transformer spectrophotometer FTIR™.

2.4. Adsorption test procedures

In order to pre-scan the adsorption efficiency of the studied adsorbents, 0.2 g of each adsorbent was added to 150 mL of chlorophenol solution (200 ppm) in 500 mL Erlenmeyer flask and stirred at 200 rpm for 4 h at 25°C. Then the medium was filtered and the concentration of the remaining chlorophenol was determined spectrophotometrically. The experiment was repeated using 1 g of the adsorbents at different conditions including: different time interval of: 30, 60, 120, 180, and 240 min, different pH of 1–8, different amount of chlorophenol (50, 100, 200, 300, and 400 ppm) and different temperature range of 30°C–70°C. Adsorption isotherm study was performed by studying the adsorption of chlorophenol at different interval times (30, 60, 120, 180, and 240 min), while the kinetic study was performed at different adsorbents weights (0.02, 0.04, 0.06, 0.08, 0.1, 0.2, 0.4, and 0.5 g). At the end, the residual adsorbents were separated, washed by bidistilled water and dried at 80°C for 24 h.

3. Results and discussion

3.1. Structure of adsorbents

The used adsorbents in this study were *Musa sapientum* (banana peel), palm leaf, and water hyacinth. These products are considered as agricultural wastes and produced in huge amounts in the environment. The bioactive components presented in *Musa sapientum* (banana peel) are crude lipid, carbohydrate, crude fibers (cellulose) [24] in addition to moderate contents of phytate, saponin, and tannin (Fig. 1), while palm leaf, and water hyacinth contains mainly cellulose, lignin, and hemicellulose [25]. The percentage of the bioactive compounds in the different adsorbents was varied as represented in Table 1. The presence of different bioactive components in the different adsorbents was confirmed through FTIR spectroscopic analyses (Figs. S1a–c).

FTIR spectra of water hyacinth showed the following absorption bands: 3,600–3,200 cm^{-1} (centered at 3,424 cm^{-1}) assigned for O–H, 2,925, 2,850 cm^{-1} allocated for symmetric and asymmetric stretching of alkyl C–H, 1,640 cm^{-1} assigned for aromatic C=C, 1,073 cm^{-1} assigned for C–O ether, 1,251 cm^{-1} attributed to C–O alcoholic, 773, 620 cm^{-1} assigned for bending of C–H aromatic (Fig. S1a).

FTIR spectra of palm leaf showed the following absorption bands: 3,600–3,200 cm^{-1} (centered at 3,435 cm^{-1}) for O–H,

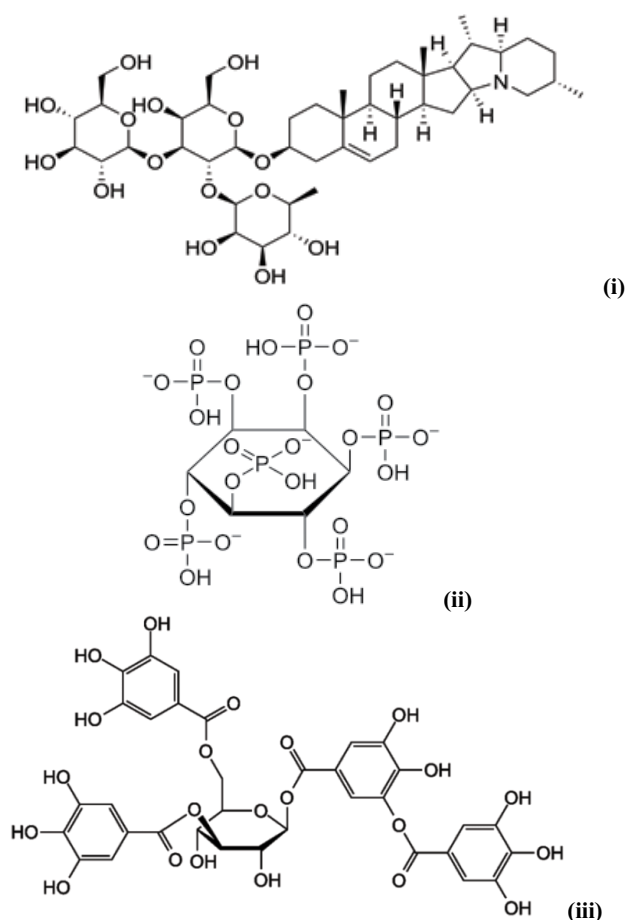


Fig. 1. Chemical structure of: (i) saponin, (ii) phytic acid, and (iii) tannin.

Table 1

Bioactive components and their average ratio in water hyacinth, palm leaf, and banana peel, and their adsorption efficiency for chlorophenol as obtained from pre-screening test

Adsorbent	Component percentage	Efficiency, %
Water hyacinth	Cellulose 31.6%	94
	Hemicellulose 27.3%	
	Lignin 4%	
Palm leaf	Cellulose 42.6%	98
	Hemicellulose 21.3%	
	Lignin 14.4%	
Banana peel	Phytate (mg/g) 0.34	99
	Saponin (mg/g) 24.3	
	Tannin 30%–40%	
	Crude lipid 1.70%	
	carbohydrate 59.0%	
	Crude fiber 31.7%	

2,921, 2,853 cm^{-1} allocated for symmetric and asymmetric stretching of alkyl C–H, 1,632 cm^{-1} assigned for aromatic C=C, 1,047 cm^{-1} assigned for C–O ether, 1,257 cm^{-1} attributed to C–O alcoholic, 770, 620 cm^{-1} of aromatic C–H bending (Fig. S1b).

FTIR spectra of *Musa sapientum* (banana peel; Fig. S1c) showed the characteristic absorption bands of cellulose and hemicellulose (broad band centered at 3,429, 1,253, 1,043 cm^{-1}), which also indicate the presence of saponin and tannin. Furthermore, additional absorption bands which were: broad band in the range of 3,600–3,000 cm^{-1} and centered at 3,500 cm^{-1} , 1,180 cm^{-1} assigned for P=O symmetrical stretching, weak band at 1,160 cm^{-1} assigned for P=O asymmetrical stretching 909 cm^{-1} assigned for P=OH symmetrical stretching, 1,010 cm^{-1} for P=OH asymmetrical stretching, representing the presence of phytate in banana peel adsorbent.

3.2. Adsorption studies

Several factors are influencing the adsorption of chlorophenol by the studied adsorbents including adsorbent amount, concentration of chlorophenol, pH of the medium, initial chlorophenol concentration, time of adsorption process and temperature. The adsorption capacity of each adsorbent at equilibrium was calculated using Eq. (1):

$$Q_e = \frac{(C_{\text{initial}} - C_{\text{final}})}{\text{wt}_{\text{ads}}} \quad (1)$$

where Q_e is the adsorption capacity (mg/g); C_{initial} is the initial concentration of chlorophenol; C_{final} is the final concentration of chlorophenol; wt_{ads} is the weight of adsorbent used. The obtained data were listed in Table 2. From the obtained data (Table 2), it is clear that the adsorption capacities of the different adsorbents were comparatively high, and the most effective and adsorptive adsorbent was *Musa sapientum* (banana peel) with adsorption capacity of 388.9 mg/g.

Table 2

Adsorption isotherm parameters obtained for adsorption process of chlorophenol using water hyacinth, palm leaf, and banana peel as adsorbents at 25°C

Adsorbent	Adsorption isotherm				Adsorption capacity, mg/g
	Langmuir		Freundlich		
	R^2	R^2	k_f , mg/g	n	
Water hyacinth	0.8879	0.9995	76.01	1.32	288.09
Palm leaf	0.8851	0.9992	114.7	1.31	290.34
Banana peel	0.9082	0.9982	482.2	1.77	388.89

3.2.1. Effect of adsorbent amount

The adsorption of pollutants from the contaminated medium by the adsorbents is occurred due to the interaction between the reactive pollutant molecules and the accessible adsorption sites in the adsorbents. The number of adsorption sites accessible for the adsorption is increased by increasing the adsorbent amount. The influence of the adsorbent amount on the removal efficiency of chlorophenol from the contaminated medium was represented graphically in Fig. 2. It is clear from Fig. 2 that the steady increase in the amount of the different adsorbents progressively increases the adsorption efficiency. The relative increase in the adsorption efficiency is assumed due to the increase in the adsorbent surface area and accessibility of additional adsorption sites [26] by increasing their amounts.

3.2.2. Effect of pH

The acidity or alkalinity of the medium influences the ionic profile of the functional groups of the adsorbents (i.e., carboxyl, phosphate, and amino groups), and the chlorophenol in the medium. Fig. 3 signifies the variation of adsorption efficiencies obtained of the studied adsorbents towards chlorophenol at different pH values (pH 5, 7, 9). It is clear that the adsorption efficiencies of the different adsorbents were increased by increasing the pH of the medium from 1 to 6, and reaches the highest values at pH = 7. In the acidic medium (pH < 7), the chlorophenol is protonated to form its cationic form as represented in Fig. 4, that leads to ionization of the hydroxyl group attached to phenyl group. Furthermore, the various hydroxyl groups on the different adsorbents are protonated, as well, to change the adsorbents surfaces into partially ionized surfaces [27]. The interaction between the partially ionized adsorbents surfaces and the chlorophenol is decreased by increasing the acidity of the medium. Also, the competition between the charged chlorophenol and the hydrogen protons in the medium [28] decreases the adsorption of the former than the later. Increasing the pH of the medium decreases the protonated form of the adsorption sites of the different adsorbents and also decreases the free hydrogen protons in the medium. That leads to spontaneous adsorption of the chlorophenol molecules to the adsorption sites of the adsorbents and consequently increases the adsorption efficiency values. At higher pH values (in the range of the alkaline), the negative charges increased on the adsorbents surface which increases

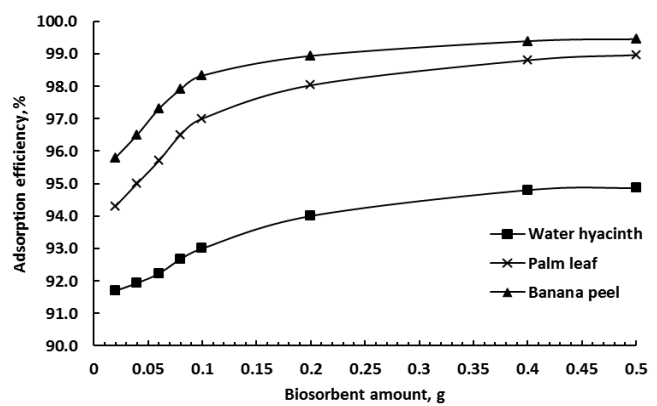


Fig. 2. Effect of adsorbent concentration on the adsorption of chlorophenol on: water hyacinth, palm leaf, and banana peel adsorbents.

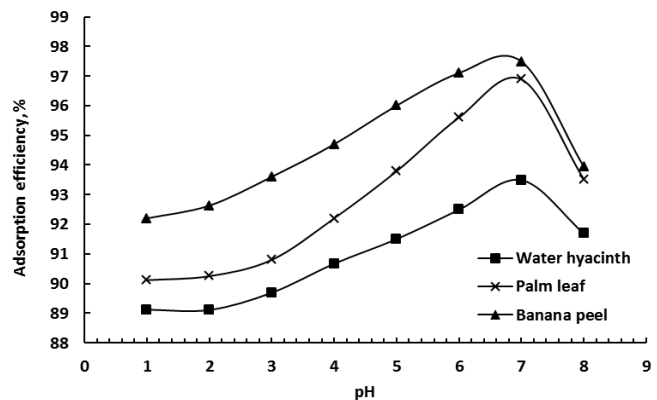


Fig. 3. Effect of pH on the adsorption of chlorophenol on water hyacinth, palm leaf, and banana peel adsorbents.

the repulsion between the chlorophenol molecules [29] and the adsorption sites, which decreases the adsorption efficiency to lower values.

3.2.3. Effect of time on adsorption process

The effect of time on adsorption efficiency removal of chlorophenol from the solution by the studied adsorbents was studied at wide contact time range of 30 to 240 min as presented in Fig. 5. The optimum adsorption efficiency

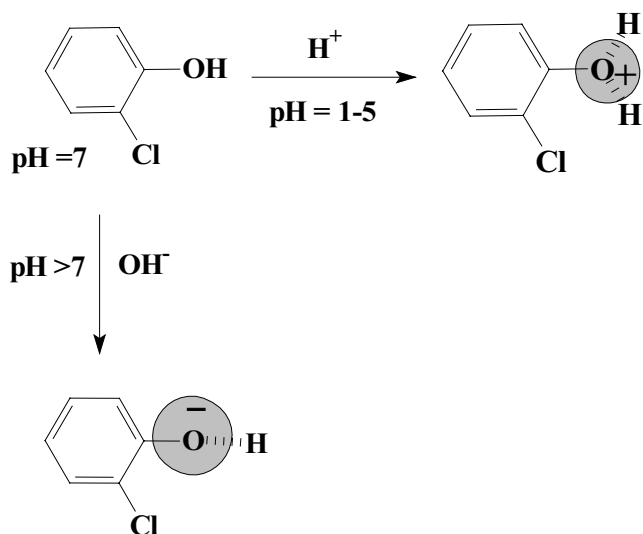


Fig. 4. Structure of chlorophenol at different pH values.

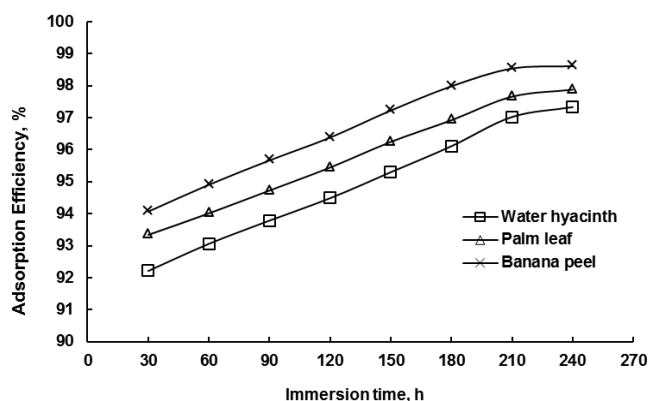


Fig. 5. Effect of immersion time on the adsorption of chlorophenol on water hyacinth, palm leaf, and banana peel adsorbents.

removal of chlorophenol was achieved at 210 min. further increase in the process duration leads to decrease in the efficiency of the adsorption process. Fig. 5 represents that the efficiency of adsorption is raised sharply in the initial process stages, indicating that there are plenty of accessible adsorption active sites. At longer process time, stability is reached in all curves indicating that the adsorbents surfaces are saturated by the adsorbed chlorophenol at this time [30]. It was observed (data not included in Fig. 5) that increasing the duration of the process more than 240 min (270–300 min) leads to decrease in the adsorption efficiency. This can be attributed to the desorption process of the adsorbed chlorophenol from the adsorbents surface.

3.2.4. Effect of initial chlorophenol concentration

The influence of chlorophenol concentration in the medium on the adsorption process was studied using constant amount of the different adsorbents in the presence of various amounts of chlorophenol in the medium (50, 100, 200, 300, and 400 ppm). Fig. 6 represents the variation of

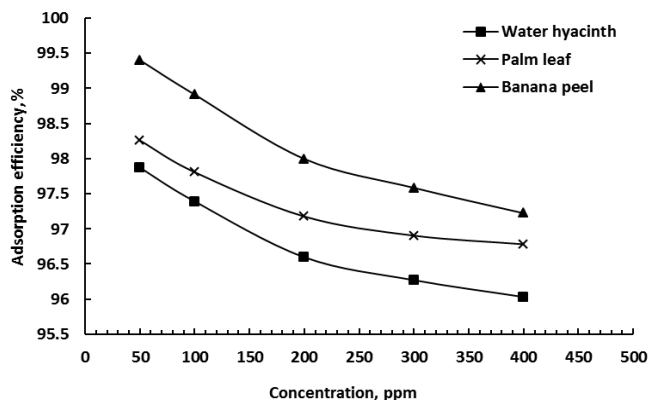


Fig. 6. Effect of initial chlorophenol concentration on the adsorption of chlorophenol on water hyacinth, palm leaf, and banana peel adsorbents.

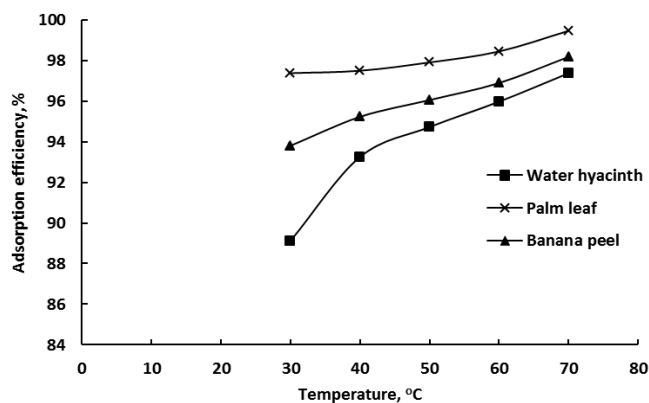


Fig. 7. Effect of temperature on the adsorption of chlorophenol on water hyacinth, palm leaf, and banana peel adsorbents.

the adsorption efficiency of the different adsorbents at a wide range of chlorophenol concentration in the medium. It is clear that the increase in the chlorophenol concentration decreases the adsorption efficiency of the three biosorbents. The decrease in the initial concentration of chlorophenol increases the number of successful collisions between its molecules and the adsorptive active sites on the surface of the adsorbents which enhances the adsorption process [31,32].

3.2.5. Effect of temperature

To determine the effect of temperature on the adsorption of chlorophenol by the studied adsorbents, experiments were conducted in a temperature range of 30°C–70°C (Fig. 7). It is clear from Fig. 7 that the gradual increase in the temperature of the medium, the adsorption efficiency of the adsorbents is gradually increased. From the adsorption profile of chlorophenol (Fig. 7), it can be concluded that the adsorption process of chlorophenol on the studied adsorbents is an endothermic process [33]. The endothermic adsorption process is enhanced by increasing the temperature of the medium. The increase in the temperature increases the swelling of the adsorbents in the aqueous medium which increases the validity of the adsorption active sites to interact by the chlorophenol

molecules. Furthermore, increasing the temperature increases the collision between the dispersed chlorophenol molecules in the medium and the available adsorption sites [34]. These two reasons increase the adsorption efficiency of the studied adsorbents at higher temperatures.

3.3. Adsorption isotherm models

Sorption equilibrium can be described by a number of models available in the literature. In this work, two models were applied to obtain the suitable adsorption isotherm model which describes the adsorption of chlorophenol on the studied adsorbents, Langmuir model and Freundlich model.

Langmuir model assumes that the adsorption process formed a monolayer of the solute (chlorophenol) on the surface of the adsorbents. The surface consisted of a limited number of identical sites with homogeneous adsorption energy, and the adsorbed molecules are adsorbed uniformly on the surface. This model [35] is expressed using Eq. (2):

$$\frac{C_e}{q_e} = \frac{1}{q_{\max} K_L} + \frac{C_e}{q_{\max}} \quad (2)$$

where C_e is the concentration of chlorophenol in the solution (mg/L) when equilibrium is reached, q_e is the amount of chlorophenol adsorbed per mass unit of adsorbent at equilibrium (mg/g), q_{\max} is the uptake capacity when the adsorbent surface is completely covered with chlorophenol molecules (maximum uptake capacity; mg/g), K_L is the Langmuir adsorption constant that represents the affinity between the adsorbents and the chlorophenol molecules.

Freundlich isotherm is an empirical expression that takes into consideration the heterogeneity of the adsorbent surface and formation of multilayer of chlorophenol molecules to adsorptive active sites on the adsorbent surface. Freundlich model is expressed in Eq. (3) [36]:

$$\ln q_e = \frac{1}{n} \ln C_e + \ln K_f \quad (3)$$

where K_f is the Freundlich adsorption constant.

The plot based on Langmuir isotherm model for the adsorption of chlorophenol on the studied adsorbents (Fig. S2) was used to calculate Langmuir adsorption parameters and were listed in Table 2. The correlation coefficients obtained from Langmuir adsorption profile were ranged between 0.8851 and 0.9082 (Table 2). Based on the correlation coefficients values of Langmuir adsorption model, one can determine the unavailability of this model to describe the adsorption of chlorophenol molecules on the studied adsorbents. That can be related to the type of adsorption of these molecules on the adsorbents and the formation of multilayer on the surface, in addition to the heterogeneity of the adsorbent surface [37].

Freundlich adsorption isotherm was applied to the obtained data of adsorption of chlorophenol using the studied adsorbents and the isotherm profile was represented in Fig. 8. The isotherm parameters were obtained and their values were listed in Table 2. It is clear from data in Table 2 related to Freundlich adsorption isotherm that the correlation coefficient values (R^2) are ranged between 0.9982 and

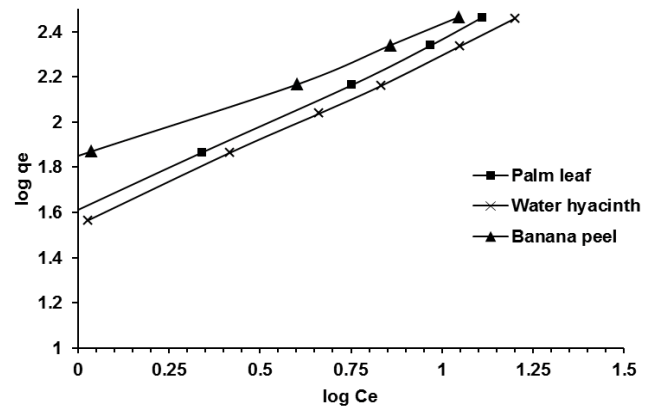


Fig. 8. Freundlich adsorption isotherm of chlorophenol on water hyacinth, palm leaf, and banana peel adsorbents.

0.9995. That showed the validity of Freundlich adsorption isotherm in describing the adsorption process of chlorophenol on the studied adsorbents. Based on Freundlich adsorption isotherm, the chlorophenol molecules are adsorbed on the studied adsorbent nonhomogeneously due to the different adsorptive sites energies, and the adsorbed molecules are arranged in a multilayer form. Freundlich adsorption isotherm gave k_f and n parameters. k_f is correlated to the maximum adsorption capacity of the adsorbents, and represents the highest adsorbed amount on adsorbent at equilibrium. n signifies the adsorption strength on the adsorbent. n value from 1 to 10 indicates relatively strong adsorption. The obtained n values in the studied biosorbents were more than 1, which indicates relatively strong adsorption of chlorophenol molecules on the adsorbents [38]. The maximum adsorption capacities of the studied adsorbents were 76, 114.7, and 483.2 mg/g, indicating their high performance in the removal of chlorophenol from the medium.

3.4. Kinetics of adsorption process

Several adsorption kinetic models such as pseudo-first-order and pseudo-second-order kinetic models were applied to recognize the adsorption kinetics and the rate determining steps of the adsorption process. The rate determining steps may include diffusion control, chemical reactions and particle diffusion [38]. The pseudo-first-order kinetic model was rationalized in Eq. (4):

$$\log(q_e - q_t) = \log q_e - \frac{k_1}{2.303} t \quad (4)$$

where q_e and q_t are the amounts of chlorophenol adsorbed onto the biosorbents (mg/g) at equilibrium and at time t , respectively, and k_1 is the rate constant of pseudo-first-order model (min^{-1}).

This model describes the proportional relationship between the rate of adsorption and the number of unoccupied sites of the adsorbents. This model can be applied for the short time adsorption process, due to the adsorptive active sites stayed unoccupied at the first stages of the adsorption process. Ho and McKay [39] noticed that the use of the

Table 3

Kinetic parameters of pseudo-first- and pseudo-second-order and intraparticle diffusion model of adsorption by water hyacinth, palm leaf, and banana peel as adsorbents at 25°C

Adsorbent	Pseudo-first-order			Pseudo-second-order			Intraparticle diffusion		
	R^2	q_e	k_2	R^2	k_{int1} (mg/g min ^{1/2})	R^21	k_{int2} (mg/g min ^{1/2})	R^22	
Water hyacinth	0.9373	99.34	0.011	0.999	0.465	0.997	0.865	0.997	
Palm leaf	0.9360	107.14	0.010	0.999	0.4309	0.988	0.708	0.998	
Banana peel	0.9163	110.29	0.009	0.999	0.474	0.996	0.495	0.921	

pseudo-first-order model for estimation of the adsorption kinetics is not suitable for longer time adsorption process.

The pseudo-second-order kinetic model predicts the rate determining step of the adsorption process and the bonds nature between the adsorbents and the adsorbed molecules according to Eq. (5):

$$\frac{t}{q_t} = \frac{1}{k_2 q_e^2} + \frac{1}{q_e} t \quad (5)$$

where k_2 is the second order rate constant (g mg⁻¹ min⁻¹).

The pseudo-first-order kinetic model for the adsorption of chlorophenol on the studied adsorbents was plotted (Fig. S3), while its corresponding extracted data were listed in Table 3. It is clear that the model is applicable at the first stages of the adsorption process, but it is inapplicable for longer times. Furthermore, the comparatively low correlation coefficients of the model and the negative slopes of the profiles indicate that the model is indescribable for the adsorption process.

Fig. 9 represents the profile representation of the adsorption data of the chlorophenol-adsorbents systems at 25°C using pseudo-second-order kinetic model. The kinetic data including the correlation coefficients (R^2), equilibrium concentration (q_e), and rate constant (k_2) of the adsorption process were extracted and listed in Table 3. It is obvious from the data obtained from the pseudo-second-order kinetic model that the correlation coefficients are ranged between 0.9998 and 0.9999 (i.e., ≈ 1), which indicates the suitability of the kinetic model in description of the adsorption process kinetics. The theoretical values of the equilibrium concentrations (q_e ; Table 3) were comparable with the experimental values (Table 1) obtained from the experimental measurements. The model provides good description for the adsorption process along the whole time range. Also, the adsorption process occurred by physical binding [40,41] between the adsorbents functional groups (adsorptive sites) and the chlorophenol molecules through their lone pairs of electrons.

The adsorption process on a porous adsorbent will generally have multi-step process. These steps involve the transport of the targeted molecules from the bulk of the solution, film diffusion, intraparticle diffusion in the pores and in the solid phase, and finally adsorption on the reactive sites. It is likely that the intraparticle diffusion is the rate controlling step in a well stirred batch system. The intraparticle diffusion model is given by Eq. (6) [42]:

$$q_t = k_{int} t^{1/2} \quad (6)$$

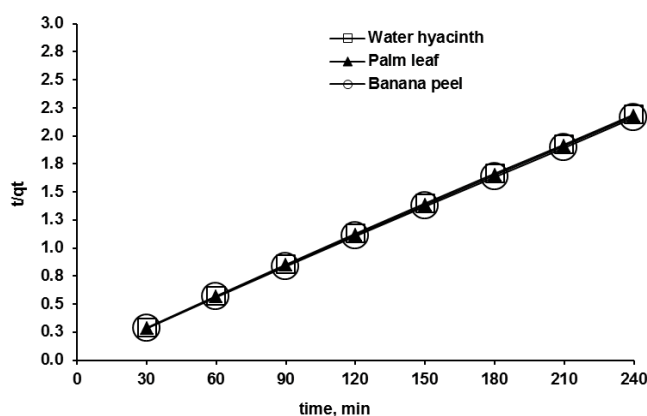


Fig. 9. Pseudo-second-order kinetic model of adsorption of chlorophenol on water hyacinth, palm leaf, and banana peel adsorbents.

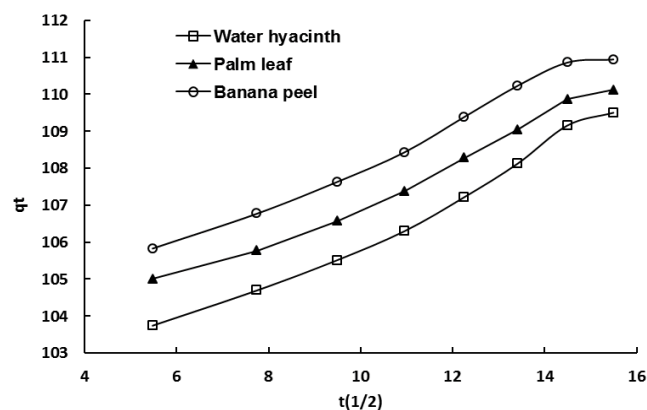


Fig. 10. Intraparticle diffusion kinetic model of adsorption of chlorophenol on water hyacinth, palm leaf, and banana peel adsorbents.

where q_t is the amount of chlorophenol adsorbed by the studied adsorbents in mg/g after t time, k_{int} is the rate constant of intraparticle diffusion step in mg/g min^{1/2}.

The straight line plots of q_t against $t^{1/2}$ were used to determine the intraparticle diffusion rate (k_{int}) and correlation coefficient (R^2). Based on Fig. 10, the plot showed multi-linearity regions indicating the two-step adsorption process occurred during the adsorption process. The first linear region was followed by a plateau region. The initial linear region represented the intraparticle diffusion while the plateau region corresponds to equilibrium. The straight line did not pass

the origin indicating that the intraparticle diffusion is not the exclusive rate limiting process [43]. The correlation coefficients obtained (Table 3) showed a good fit for both regions whereas the first intraparticle diffusion rate constant ($k_{int,1}$) signifies the first linear region at short time, while $k_{int,2}$ represents the equilibrium region.

3.4.1. Boyd equation

To determine if film or particle diffusion step controls the adsorption rate on the adsorbent, Boyd model was applied in Bt vs. time adsorption profile of chlorophenol using the tested adsorbents. It was reported that Boyd equation can be applied to determine the rate-controlling step for adsorbents [44,45] and expressed as Eq. (7):

$$F = 1 - \left(\frac{6}{\pi^2} \right) \exp(-Bt) \quad (7)$$

where Bt is the function of F and F is the fraction of chlorophenol adsorbed at different times, t . The F value can be calculated using Eq. (8):

$$F = \frac{q_t}{q_e} \quad (8)$$

where q_t and q_e are the amount of adsorbed chlorophenol on adsorbents at any time t and at equilibrium, respectively.

The Bt values at different contact times (t) can be calculated using Eq. (9) in the case of $F > 0.85$ [45]:

$$Bt = -0.4997 - \ln(1 - F) \quad (9)$$

On the basis of Bt -contact time profile, the plot of Boyd model can be obtained (Fig. 11). It was suggested that if the plot of Bt vs. t is a straight line and passes through the origin, it is the pore diffusion that controls the rate of mass transfer (or particle diffusion mechanism) [46,47]. In contrast, if the plot is nonlinear or linear but does not pass through the origin, film-diffusion or external mass transport is the

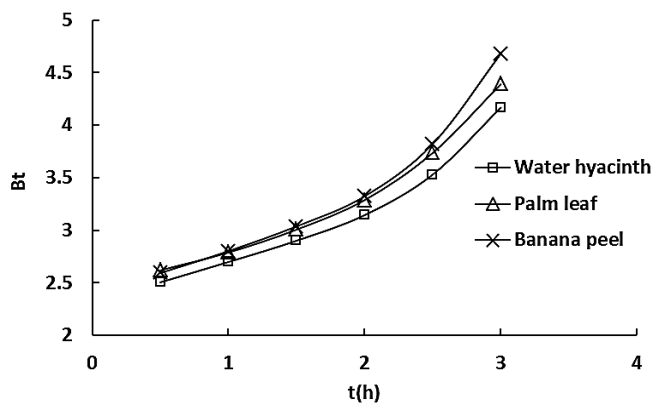


Fig. 11. Plot of Boyd model for the adsorption of chlorophenol on water hyacinth, palm leaf, and banana peel adsorbents.

dominating step. Fig. 11 presents the plot of Boyd model for the adsorption of chlorophenol on the studied adsorbents. As shown in Fig. 11, it can be noted that the curves are all nonlinear and do not pass through the origin. Based on these findings, it can be concluded that the adsorption of chlorophenol on the studied adsorbents is a film-diffusion mechanism.

3.5. Adsorption mechanism of chlorophenol on the adsorbents

The mechanism of adsorption of the chlorophenol molecules on the studied adsorbents was determined using two main data in the study.

First, the nature of the bonds between the chlorophenol molecules and the adsorbents surface was determined chemically using FTIR spectra of the unloaded and loaded

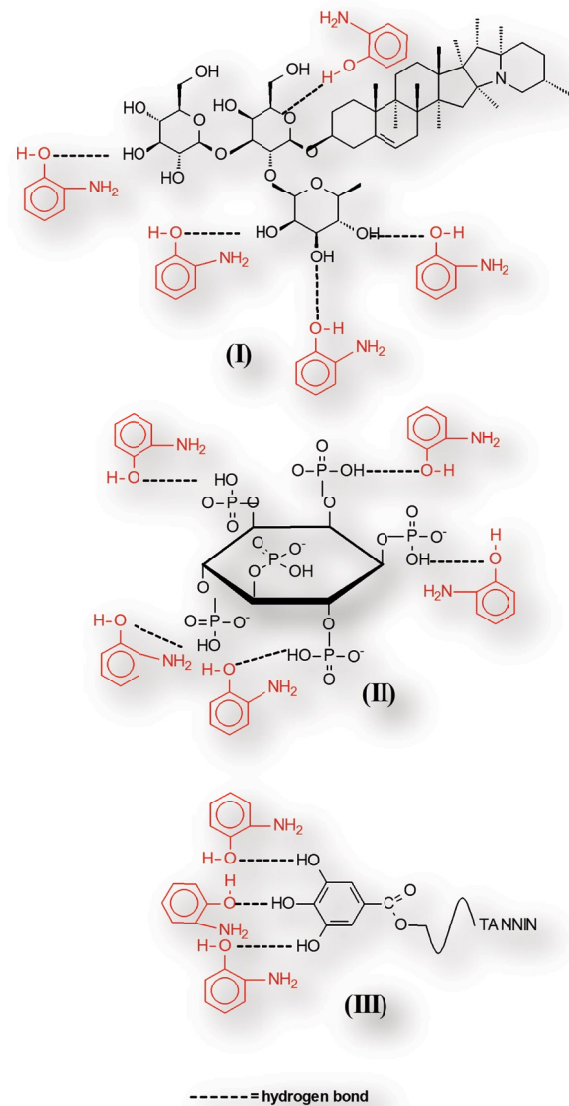


Fig. 12. Representative mechanism for adsorption of 2-chlorophenol on the different bioactive components (I: saponin, II: phytic acid, and III: tannin) in the studied adsorbents.

adsorbents by chlorophenol molecules. The characteristic absorption bands of the different unloaded adsorbents (Figs. S1 a–c) were compared by their wavenumber in the case of the loaded adsorbents by chlorophenol molecules (Figs. S4 a–c). Generally, all the absorption bands of the polar groups (C–O, O–H, C–O–C, P=OH, P=O) in the cellulose, hemicellulose, lignin, tannin, saponin, and phytate bioactive components were shifted to lower wavenumbers. That indicates the interaction between the chlorophenol molecules and these polar groups. The interaction between the adsorbents and the chlorophenol seems to be physical interaction due to the values of the shifts were ranged between 10 and 20 cm^{-1} .

Second, the adsorption studies showed that the adsorbed chlorophenol molecules are attached to the adsorbents on the different polar sites (according to Freundlich model). These polar sites (adsorptive sites) are C–O, O–H, C–O–C, P=OH, and P=O groups.

Finally, the kinetic studies showed that the adsorbed molecules are forming several layers on the adsorbents surface in the form of a film, which indicates the presence of interaction between the chlorophenol molecules on the adsorbents surfaces. Fig. 12 represents the proposed attachment of the adsorbed chlorophenol molecules on the studied adsorbents.

3.6. Cost analysis of the treatment

The cost study includes the cost of the adsorbents and their collection, processing of the adsorbents in the suitable form, treatment cost and final output. The cost of adsorbents collection is 20 \$/ton; cost of adsorbents drying and processing is 45 \$/ton. The total cost of ready-to-use adsorbent is 65 \$/ton. The average removal of chlorophenol by one ton of ready-to-use adsorbent is 300 kg. Therefore, the final cost of processing 1 kg of adsorbent is 6.5 cent. Considering that the concentration of chlorophenol in wastewater is 150 mg/L. Consequently, the cost of treatment of 1 L of wastewater is less than 8 cent per one liter of wastewater.

4. Conclusions

- Agricultural wastes can be used for remediation of chlorophenol from wastewater.
- The process follows Freundlich isotherm and pseudo-second-order kinetic model.
- The process occurred via several steps ended by equilibrium at adsorbent surface.
- Banana peel has the highest removal efficiency due to its bioactive components.
- Adsorption of chlorophenol on the tested adsorbents is film diffusion mechanism.

References

- [1] X. Sun, C. Wang, Y. Li, W. Wang, J. We, Treatment of phenolic wastewater by combined UF and NF/RO processes, *Desalination*, 355 (2015) 68–74.
- [2] P. Kazemi, M. Peydayesh, A. Bandegi, T. Mohammadi, O. Bakhtiari, Stability and extraction study of phenolic wastewater treatment by supported liquid membrane using tributyl phosphate and sesame oil as liquid membrane, *Chem. Eng. Res. Des.*, 92 (2014) 375–383.
- [3] S. Mohammadi, A. Kargari, H. Sanaeepur, K. Abbassian, A. Najafi, E. Mofarrah, Phenol removal from industrial wastewaters: a short review, *Desal. Wat. Treat.*, 53 (2015) 2215–2234.
- [4] A. Eslami, M. Hashemi, F. Ghanbari, Degradation of 4-chlorophenol using catalyzed peroxymonosulfate with nano-MnO₂/UV irradiation: toxicity assessment and evaluation for industrial wastewater treatment, *J. Cleaner Prod.*, 195 (2018) 1389–1397.
- [5] EPA 2008 Toxic Release Inventory National Analysis. Available from: <http://www.epa.gov/> (Accessed December 2015).
- [6] S. Mukherjee, B. Basak, B. Bhunia, A. Dey, B. Mondal, Potential use of polyphenol oxidases (PPO) in the bioremediation of phenolic contaminants containing industrial wastewater, *Rev. Environ. Sci. Biotechnol.*, 12 (2013) 61–73.
- [7] V. Peings, J. Frayret, T. Pigot, Mechanism for the oxidation of phenol by sulfatoferrate (VI): comparison with various oxidants, *J. Environ. Manage.*, 157 (2015) 287–296.
- [8] Z. Tasic, V.K. Gupta, M.M. Antonijevic, The mechanism and kinetics of degradation of phenolics in wastewaters using electrochemical oxidation, *Int. J. Electrochem. Sci.*, 9 (2014) 3473–3490.
- [9] U. Ghimire, M. Jang, S.P. Jung, D. Park, Electrochemical Removal of Ammonium Nitrogen and COD of Domestic Wastewater using Platinum Coated Titanium as an Anode Electrode, *Energies*, 12 (2019) 1–13.
- [10] I. Pookpoosa, R. Jindal, D. Morknuy, K. Tantrakarnapa, Occurrence and efficacy of Bisphenol A (BPA) treatment in selected municipal wastewater treatment plants, Bangkok, Thailand, *Water Sci. Technol.*, 72 (2015) 463–471.
- [11] A.M. Orozco, E.M. Contreras, N.E. Zaritzky, Biodegradation of Bisphenol A and its metabolic intermediates by activated sludge: stoichiometry and kinetics analysis, *Int. Biodeterior. Biodegrad.*, 106 (2016) 1–9.
- [12] A. Steevensz, L.G. Villegas, W. Feng, K.E. Taylor, J.K. Bewtra, N. Biswas, Soybean peroxidase for industrial wastewater treatment, *J. Environ. Eng. Sci.*, 9 (2014) 181–186.
- [13] G. Islamuddin, M.A. Khalid, S.A. Ahmad, Study of eco-friendly agricultural wastes as non-conventional low cost adsorbents: a review, *Ukrainian J. Ecol.*, 9 (2019) 68–75.
- [14] N.A. Hikmat, B.B. Qassim, M.T. Khethi, Thermodynamic and kinetic studies of lead adsorption from aqueous solution onto petiole and fiber of palm tree, *Am. J. Chem.*, 4 (2014) 116–124.
- [15] A.A. Bakr, N.A. Sayed, T.M. Salama, I.O. Ali, R.R. Abdel Gayed, N.A. Negm, Potential of Mg-Zn-Al layered double hydroxide (LDH)/montmorillonite nanocomposite in remediation of wastewater containing manganese ions, *Res. Chem. Intermed.*, 44 (2018) 389–405.
- [16] E. Demirbas, N. Dizge, M.T. Sulak, M. Koby, Adsorption kinetics and equilibrium of copper from aqueous solutions using hazelnut shell activated carbon, *Chem. Eng. J.*, 148 (2009) 480–487.
- [17] N.M. Mahmoodi, B. Hayati, H. Bahrami, M. Arami, Dye adsorption and desorption properties of Menthapulegium in single and binary systems, *J. Appl. Polym. Sci.*, 122 (2011) 1489–1499.
- [18] R. Mukherjee, S. De, Adsorptive removal of phenolic compounds using cellulose acetate phthalate–alumina nanoparticle mixed matrix membrane, *J. Hazard. Mater.*, 265 (2014) 8–19.
- [19] J.A. Oliveira, F.A. Cunha, L.A.M. Ruotolo, Synthesis of zeolite from sugarcane bagasse fly ash and its application as a low-cost adsorbent to remove heavy metals, *J. Cleaner Prod.*, 229 (2019) 956–963.
- [20] V.S. Tran, H.H. Ngo, W. Guo, J. Zhang, S. Liang, C. That, Typical low cost biosorbents for adsorptive removal of specific organic pollutants from water, *Bioresour. Technol.*, 182 (2015) 353–63.
- [21] S.K. Nadavala, H.M. Che, H.S. Woo, Biosorption of phenolic compounds from aqueous solutions using pine (*Pinus densiflora* Sieb) bark powder, *BioResources*, 9 (2015) 5155–5174.
- [22] M. Masomi, A.A. Ghoreyshi, G.D. Najafpour, A.R. Mohamed, Adsorption of phenolic compounds onto the activated carbon synthesized from pulp and paper mill sludge: equilibrium isotherm, kinetics, thermodynamics and mechanism studies, *Int. J. Eng. Trans. A Basicsm*, 27 (2014) 1485–1494.

- [23] A.M. Bernal, F. Gómez, L. Giraldo, J.C. Pirajá, Chemical modification of activated carbons and its effect on the adsorption of phenolic compounds, *Ing. Compet.*, 17 (2015) 109–119.
- [24] B.A. Anhwange, T.J. Ugye, T.D. Nyiaatagher, Chemical composition of *Musa sapientum* (Banana) peels, *EJEAFChem*, 8 (2009) 437–442.
- [25] M. Balat, Production of bioethanol from lignocellulosic materials via the biochemical pathway: a review, *Energy Convers. Manage.*, 52 (2011) 858–875.
- [26] M.A. Badawi, N.A. Negm, M.T.H. Abou Kana, H.H. Hefni, M.M. Abdel Moneem, Adsorption of aluminum and lead from wastewater by chitosan-tannic acid modified biopolymers: isotherms, kinetics, thermodynamics and process mechanism, *Int. J. Biol. Macromol.*, 99 (2017) 465–476.
- [27] N.A. Negm, M.G. Abd El Wahed, A.R.A. Hassan, M.T.H. Abou Kana, Feasibility of metal adsorption using brown algae and fungi: effect of biosorbents structure on adsorption isotherm and kinetics, *J. Mol. Liq.*, 264 (2018) 292–305.
- [28] A.W. Krowiak, R.G. Szafran, S. Modelski, Biosorption of heavy metals from aqueous solutions onto peanut shell as a low-cost biosorbent, *Desalination*, 265 (2011) 126–134.
- [29] M. Arami, N.Y. Limaee, N.M. Mahmoodi, N.S. Tabrizi, Equilibrium and kinetics studies for the adsorption of direct and acid dyes from aqueous solution by soymeal hull, *J. Hazard. Mater.*, 135 (2006) 171–179.
- [30] O.A. Ekpete, M. Horsfall, A.I. Spiff, Removal of chlorophenol from aqueous solution using fluted pumpkin and commercial activated carbon, *Asian J. Nat. Appl. Sci.*, 1 (2012) 96–105.
- [31] R. Slimani, I. El Ouahabi, F. Abidi, M. El Haddad, A. Regti, M.R. Laamari, S. El Antri, S. Lazar, Calcined eggshells as a new biosorbent to remove basic dye from aqueous solutions: thermodynamics, kinetics, isotherms and error analysis, *J. Taiwan Inst. Chem. Eng.*, 45 (2014) 1578–1587.
- [32] I. Hachoumi, I. El Ouahabi, R. Slimani, B. Cagnon, M. El Haddad, S. El Antri, S. Lazar, Adsorption studies with a new biosorbent *Ensis siliqua* shell powder for removal two textile dyes from aqueous solution, *J. Mater. Environ. Sci.*, 8 (2017) 1448–1459.
- [33] A. Bhatnagar, A.K. Jain, A comparative adsorption study with different industrial wastes as adsorbents for the removal of cationic dyes from water, *J. Colloid. Interface Sci.*, 281 (2005) 49–55.
- [34] Y.S. Al Degs, M.I. El Barghouthi, A.H. El Sheikh, G.M. Walker, Effect of solution pH, ionic strength, and temperature on adsorption behavior of reactive dyes on activated carbon, *Dyes Pigm.*, 77 (2008) 16–22.
- [35] S. Saleh, K.B. Kamarudin, W.A. Wan, K. Ghani, L.S. Kheang, Removal of organic contaminant from aqueous solution using magnetic biochar, *Procedia Eng.*, 148 (2016) 228–235.
- [36] Z. Aksu, Determination of the equilibrium, kinetic and thermodynamic parameters of the batch biosorption of Ni (II) onto *Chlorella vulgaris*, *Proc. Biochem.*, 38 (2002) 89–99.
- [37] E. Guibal, L. Dambies, C. Milot, J. Roussy, Influence of polymer structural parameters and experimental condition on metal sorption by chitosan, *Polym. Int.*, 48 (1999) 671–680.
- [38] Y.H. Li, Z. Di, J. Ding, D. Wu, Z. Luan, Y. Zhu, Adsorption thermodynamic, kinetic and desorption studies of Pb²⁺ on carbon nanotubes, *Water Res.*, 39 (2005) 605–609.
- [39] Y.S. Ho, G. McKay, Comparison of chemisorption kinetic models applied to pollutant removal on various sorbents, *Trans. Inst. Chem. Eng.*, 76 (1998) 332–340.
- [40] G. Crini, P.M. Badot, Application of chitosan, a natural aminopolysaccharide, for dye removal from aqueous solutions by adsorption processes using batch studies: a review of recent literature, *Prog. Polym. Sci.*, 33 (2008) 399–447.
- [41] M. Hasan, A.L. Ahmad, B.H. Hameed, Adsorption of reactive dye onto cross linked chitosan/oil palm ash composite beads, *Chem. Eng. J.*, 136 (2008) 164–172.
- [42] A.J. Varma, S.V. Deshpande, J.F. Kennedy, Metal complexation by chitosan and its derivatives: a review, *Carbohydr. Polym.*, 55 (2004) 77–93.
- [43] A. Ozcan, E.M. Oncu, A.S. Ozcan, Kinetics, isotherm and thermodynamic studies of adsorption of Acid Blue-193 from aqueous solutions onto natural sepiolite, *Colloids Surf., A*, 277 (2006) 90–97.
- [44] M.P. Tavlieva, S.D. Genieva, V.G. Georgieva, L.T. Vlaev, Kinetic study of brilliant green adsorption from aqueous solution onto white rice husk ash, *J. Colloid Interface Sci.*, 409 (2013) 112–122.
- [45] B.H. Hameed, M.I. El-Khaiary, Equilibrium, kinetics and mechanism of malachite green adsorption on activated carbon prepared from bamboo by K₂CO₃ activation and subsequent gasification with CO₂, *J. Hazard. Mater.*, 157 (2008) 344–351.
- [46] L.C. Jensen, J.R. Becerra, J.P. Rivero, M. Escudey, L. Barrientos, V.C. Castillo, Sorption kinetics of diuron on volcanic ash derived soils, *J. Hazard. Mater.*, 261 (2013) 602–613.
- [47] D. Reichenberg, Properties of ion exchange resins in relation to their structure, III: kinetics of exchange, *JACS*, 75 (1953) 589–597.

Supplementary information:

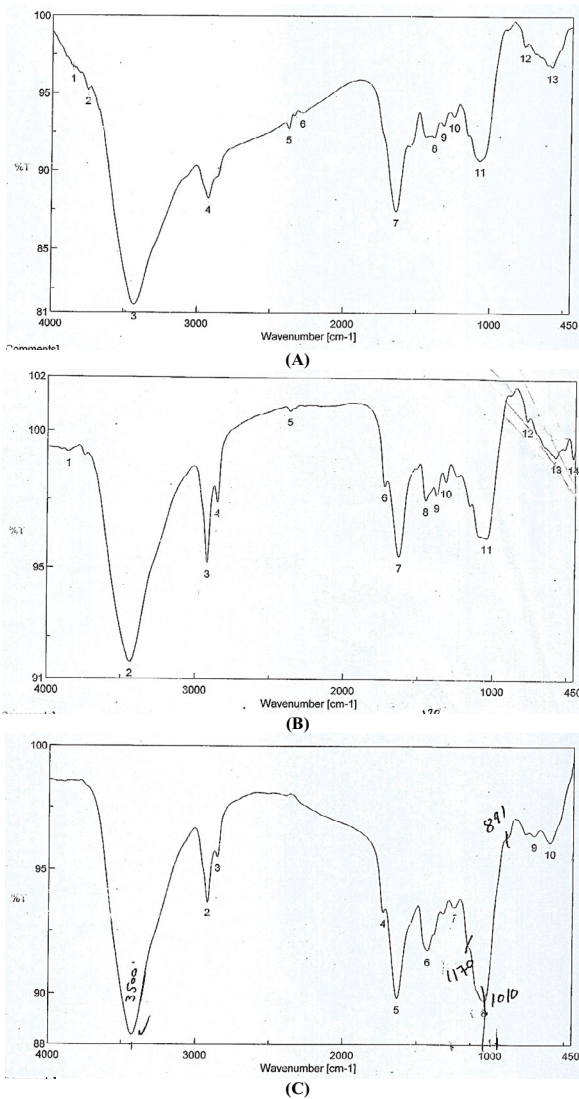


Fig. S1. FTIR spectra of pure: (a) water hyacinth, (b) palm leaf, and (c) *Musa sapientum* (banana peel).

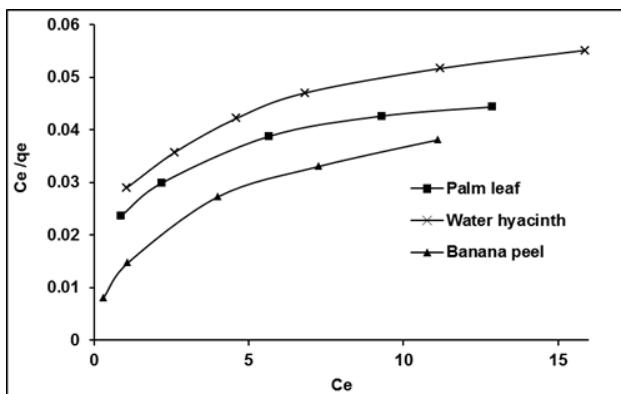


Fig. S2. Langmuir adsorption isotherm of chlorophenol on A, B, C adsorbents.

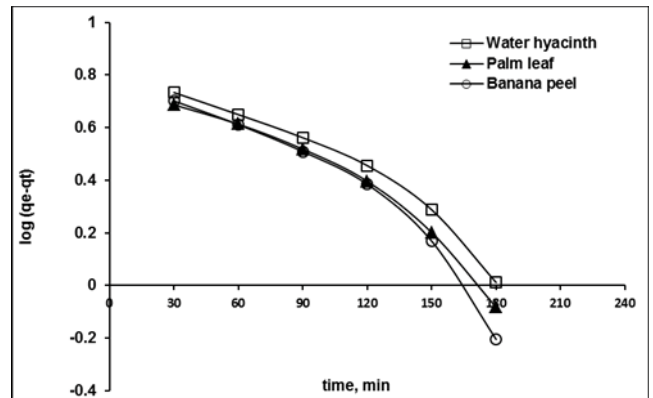


Fig. S3. Pseudo-first-order kinetic model.

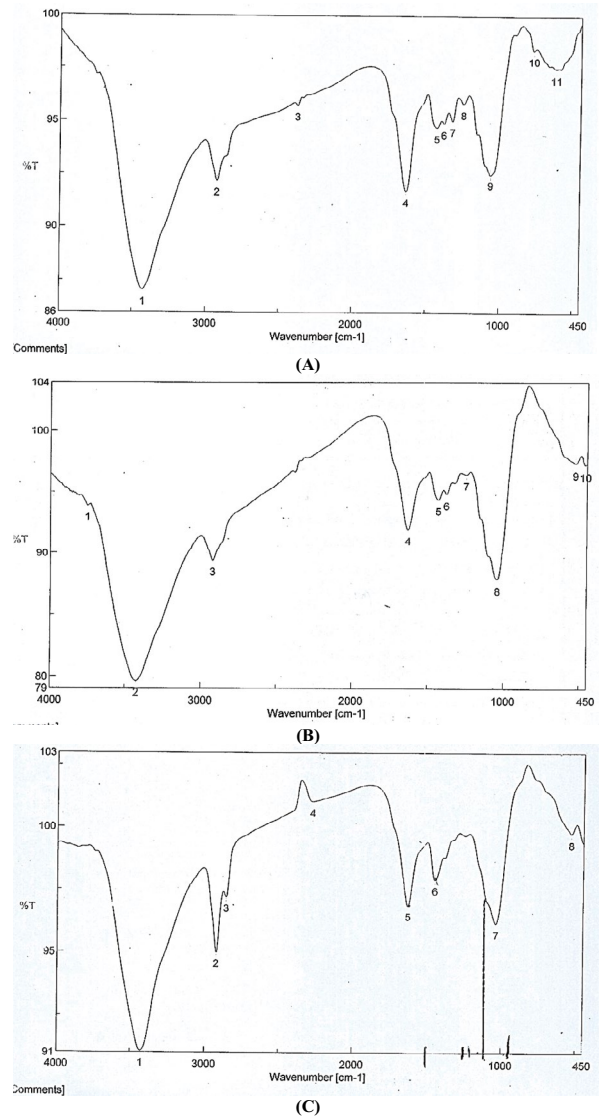


Fig. S4. FTIR spectra of chlorophenol loaded on: (a) water hyacinth, (b) palm leaf, and (c) *Musa sapientum* (banana peel).